

## Megamasers

---

**Ylva Pihlström\***

*University of New Mexico, USA*

*E-mail: ylva@unm.edu*

Very luminous extragalactic masers are commonly denoted megamasers. To date, the known megamaser sources are dominated by detections of maser emission from H<sub>2</sub>O and OH molecules. High-resolution studies of H<sub>2</sub>O and OH megamasers have been used to map the sub-parsec and parsec-scale structure in active galactic nuclei and starbursting galaxies. Other interesting uses of megamasers might be as probes of galaxies in the early universe, and as tools to measure geometric distances to galaxies. The aim of this review, particularly emphasizing high-resolution observations, is to give an overview of the scientific progress in the field on megamasers and the connection to their host galaxies.

*The 8th European VLBI Network Symposium  
September 26-29, 2006  
Toruń, Poland*

---

\*Speaker.

## 1. Introduction

Extragalactic masers often display luminosities exceeding those of Galactic masers by six orders of magnitude, hence their common notation “megamasers”. Emission from several different molecules has been identified as extragalactic masers, for example 6 cm  $\text{H}_2\text{CO}$  in Arp 220 [2, 1]. However, the large majority of megamasers have been detected in either the OH 1.6-GHz lines, or the 22-GHz  $\text{H}_2\text{O}$  line. To date, these are the maser lines that extragalactic maser research has focused upon, and they are therefore the maser species that will be considered in this review.

At a first glance, there appear to be a couple of similarities between the bright  $\text{H}_2\text{O}$  and OH megamasers: both are strongly associated with the nuclear regions of their host galaxies, and both are probes of high-density regions. However, a more detailed view will reveal a number of significant differences. Surveys have shown that the host galaxies of the two species are quite different, with intense starbursts hosting the OH megamasers and Active Galactic Nuclei (AGN) hosting the  $\text{H}_2\text{O}$  megamasers. Moreover, high spatial resolution observations have revealed that the spatial distribution is different:  $\text{H}_2\text{O}$  masers are found on pc-scale distances from the galaxy nucleus, whereas OH megamasers are found on scales of the order of 100 pc. The details of their pumping mechanisms appear quite different as well: OH megamasers are most likely radiatively pumped by infrared photons, while water megamasers are likely to be collisionally pumped. In the following sections, we will therefore discuss the OH (Sect. 2) and  $\text{H}_2\text{O}$  (Sect. 3) megamasers separately. Other informative reviews of megamasers have been published by [43, 17, 35] and [28].

## 2. OH megamasers

The first OH megamaser discovered was a putative source of a bright and broad OH emission in Arp 220 [3]. This detection triggered a number of extragalactic OH maser surveys, but it was not until the launch of the IRAS satellite that the connection between the host galaxy IR colour and OH megamasers became clear. With better search criteria, the OH megamaser detection rates started to increase. Searches for OH emission in bright IRAS sources have established several facts regarding OH megamasers. Firstly, it is clear that OH megamasers are hosted by major mergers (i.e. mergers between two gas rich spirals), in particular Ultra Luminous Infrared Galaxies (ULIRGs). Secondly, the detection rate increases with higher infrared luminosity, so that one out of three sources with far-infrared fluxes exceeding  $10^{12} L_{\odot}$  harbour an OH megamaser [18]. Thus, OH megamaser activity is strongly associated with starburst activity. Additional support for this conclusion is provided not only from work done in the radio domain [4], but also from observations at other wavelengths. For example, Chandra X-ray observations indicates that the X-ray emission in OH megamasers is consistent with starbursts, with no additional AGN component [54].

The nuclear starbursts in the ULIRGs provide a huge supply of infrared photons, which, combined with emission detected in several lines (usually the 1665-MHz and the 1667-MHz OH main lines), provide information about the pumping source. Inversion of the lines via radiative, infrared pumping was proposed soon after the OH megamaser discovery [5, 48], a scenario that was supported by several numerical calculations [36, 11].

The bulk of the OH megamaser emission has, for a long time, successfully been explained by a diffuse, foreground distribution of inverted OH molecules amplifying a background continuum [5].

The background 1.6-GHz continuum is provided from radio emission resulting from the intense starburst [16], the very same starburst that supplies the infrared pumping photons. Hence, the radio–infrared correlation for starbursts [16] combined with an unsaturated amplification process would then imply  $L_{\text{OH}} \propto L_{\text{FIR}} L_{\text{radio}} \propto L_{\text{FIR}}^2$ . Indeed, early results did point to a square relationship [5]. However, an increased sample size now shows a more linear relationship that likely indicates partly saturated maser emission [18].

The fact that OH megamasers are harboured by the nuclei of major mergers suggests that it could be possible to use them as tracers of merging activity. With more sensitive telescopes (examples of such low–frequency telescopes being either in the construction or the planning phase include the Low Frequency Array, LOFAR, and the Square Kilometer Array, SKA), it might be feasible to detect very bright OH megamasers (OH “gigamasers”) out to very high redshifts. Individual work suggests the possibility to use the OH megamasers as a tracer of the merger rate across the cosmic time, and detectabilities back to redshifts corresponding to the epoch of re-ionization [18, 10].

Interferometric studies of OH megamasers seem to have reached some consensus, indicating that the emission is distributed in 100-pc scale molecular tori surrounding the galaxy nucleus. Examples include: Mrk 231, IC 694, Mrk 273 and III Zw 35 [52, 55, 51, 46]. Figure 1 shows the results from EVN observations of Mrk 231 [42].

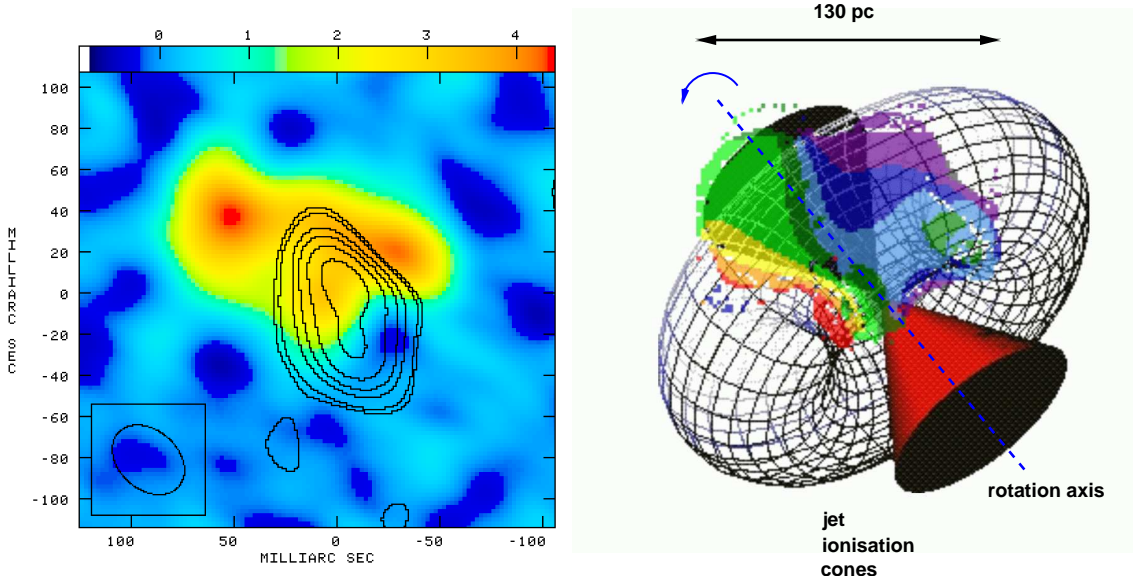


**Figure 1:** Left: The colour scale shows the distribution of the OH maser emission in Mrk 231, overlaid on the radio continuum contours outlining a Seyfert 1 nuclear structure. Right: The corresponding OH maser velocity field, which is modelled as a 100-pc scale torus [42].

At VLBI resolution, the full amount of the single-dish flux density is typically not recovered. In addition, most radio continuum associated with the nuclear starburst is resolved out. The fraction of OH maser emission that is detected appears to be concentrated in very compact components of about 1-pc size, yet the lines display significant line widths. The most studied examples of this phenomenon are: Arp 220, IRAS 17208-0014 and III Zw 35 [20, 44]. The notion, based on the observation, that part of the OH megamaser emission is very compact is further supported by

variability studies of IRAS 12032+1707. Darling & Giovanelli [19] observed significant variability in a couple of the peaks in the single-dish spectrum, and concluded that if this variation can be attributed to interstellar scintillation, sizes of the emission regions of 1 pc or less are required.

To explain the presence of pc-scale maser emission, which cannot be understood by the standard OH megamaser model, there is ongoing work both by modelling as well as new observations. On the modelling side, Parra et al. [49] have successfully used a clumpy OH torus model. A clumpy medium has amplification characteristics that significantly differ from those of a smooth medium, and as a result very compact maser emission can occur (Fig. 2).

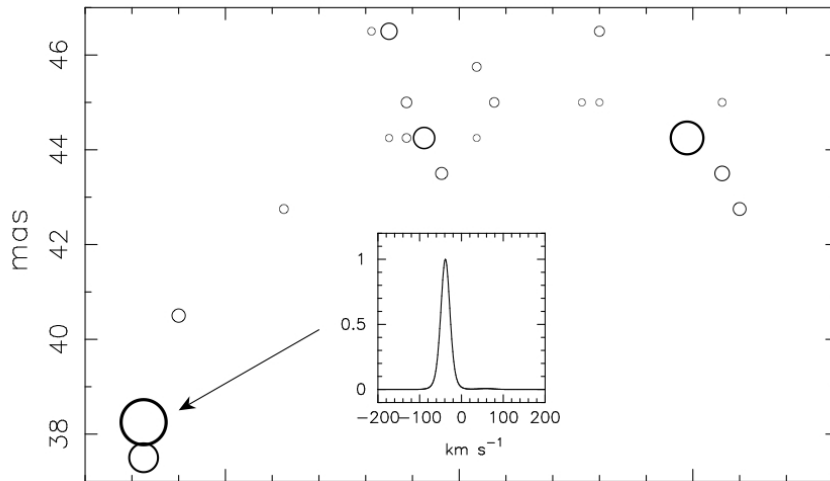


**Figure 2:** Results from modelling of a clumpy OH megamaser torus. The diameters of the circles are proportional to the velocity integrated emission. The spectrum of the brightest feature is shown in the inset [49].

Another interesting piece of work that is in progress is new high angular resolution observations of Arp 220 in OH both in emission and in absorption. Bialecki et al. [6] reported on that about 25% of the Arp 220 radio supernovae have associated OH maser emission or OH absorption, and it thus seems likely that the masers are local to, and associated with the radio supernovae. The results of these new observations, in addition to modelling efforts, are therefore providing an important, and necessary addition to the standard model.

### 3. H<sub>2</sub>O megamasers

The first H<sub>2</sub>O megamaser emission was detected in NGC 4945 [21], followed by detections in Circinus, NGC 3079, NGC 1068 and NGC 4258 [25, 37, 34, 15]. Initially, it was suspected that these H<sub>2</sub>O masers were manifestations of intense star-forming regions in the nuclear regions of the host galaxies. However, early interferometric observations ruled this out since the regions of maser emission were much more compact than expected for regions of star formation [14]. Furthermore, subsequent surveys established a strong link between H<sub>2</sub>O megamasers and AGN, in particular LINERs (Low Ionization Nuclear Emission Regions) and Seyfert 2 types (see Sect. 3.1) of AGN [9, 8, 7].

### 3.1 Accretion disk megamasers

High angular resolution observations combined with monitoring have been important to understand the geometric structure of the H<sub>2</sub>O megamasers. Several of the first VLBI observations of H<sub>2</sub>O megamasers displayed bright maser spots distributed in structures more or less perpendicular to the radio AGN nucleus. Typical single-dish spectral characteristics include two groups of “satellite” masers that in velocity domain are bracketing a group of systemic velocity masers (this feature was originally discovered in NGC 4258 by [47]). Finally, monitoring revealed velocity drifts of the maser components [33, 32]. In all, these data strongly supports that the masers arise in a sub-pc diameter disk rotating around a massive, compact object (e.g. [31]).

An obvious use of these accretion disk masers is the possibility to weigh supermassive black holes through near-Keplerian rotation curves, for instance in NGC 4258, NGC 1068 and Circinus [45, 29, 27]. Other possibilities include testing orientation-based unified schemes for AGN. These schemes suggest that different types of AGN might intrinsically be very similar, and that most observed differences are due to the viewing angle. With a typical axi-symmetric structure, the line of sight toward the central engine is more or less unobstructed in the end-on (Type 1) objects. In edge-on (Type 2) AGN, the line of sight toward the center is obscured by the circumnuclear material that probably contains the AGN fuel. Since a large fraction of the H<sub>2</sub>O megamasers arises in the accretion disks of Seyfert Type 2 AGN, they are thus likely to probe parts of the obscuring nuclear structures. VLBI mapping can provide very detailed images of the disk structure on pc and sub-pc scales. The systems mapped in detail so far indicate thin and warped disks [27, 30].

One of the more promising areas of research of H<sub>2</sub>O megamasers is the potential to measure extragalactic distances [38]. This could have a huge impact for some of the cosmological key questions, since estimates of some cosmological parameters (using analyses of the fluctuations of the cosmic microwave background) such as the equation of state of dark energy require external constraint on, for example, the Hubble constant. To single out the most plausible model from the others, an uncertainty of the Hubble constant that is less than 1% would be needed [40]. Today, the best estimate has an uncertainty of about 10%, and it is based on analysis of the period–luminosity relation in 889 Cepheids in 31 galaxies [22]. This method has its largest uncertainties in the uncertainty of the distance to the Large Magellanic Cloud, in addition to a poorly understood metallicity effect for the Cepheid period–luminosity relation. It would therefore be better to tie the extragalactic distance scale to geometric distances, in particular to a sample of reference galaxies that are distributed widely in recessional velocities and have accurate geometric distances. This is, of course, where the H<sub>2</sub>O megamasers become interesting, since VLBI mapping, monitoring and detailed modelling can be used to estimate a geometric distance [38]. NGC 4258 has been the pathfinder for this kind of work, and the most recent reported total distance uncertainty is down to 4% [41]. Tying the extragalactic distance scale to geometric distances to a large number of galaxies could have the potential to drive down the error to the 1% level [26].

### 3.2 Jet-driven megamasers

Even though most H<sub>2</sub>O megamasers are of the accretion disk type (Sect. 3.1), there are cases where the maser emission clearly does not arise in a disk. VLBI mapping has shown other structures, where the masers do not align perpendicular to the jets but instead along the jets. Examples

include: NGC 1068, NGC 1052 and Mrk 348 [24, 23, 13, 50]. In Mrk 348, a  $130 \text{ km s}^{-1}$  broad line is seen against one of the jets extending from the central engine [50]. A large line width and rapid variability suggests these masers are associated with the shocked region between the jet and the surrounding molecular gas, rather than being amplification of the background jet by random foreground clouds. Simultaneous monitoring of the maser flux density and the continuum flux density shows that the two follow each other very closely. The most straightforward explanation is that the maser and the continuum flux density variability are manifesting the same events, most likely ejection of new radio jet components. The spectra of these megamasers do not display satellite lines (as is seen in the accretion disk megamaser spectra), which might be a way to identify newly discovered jet-driven megamasers.

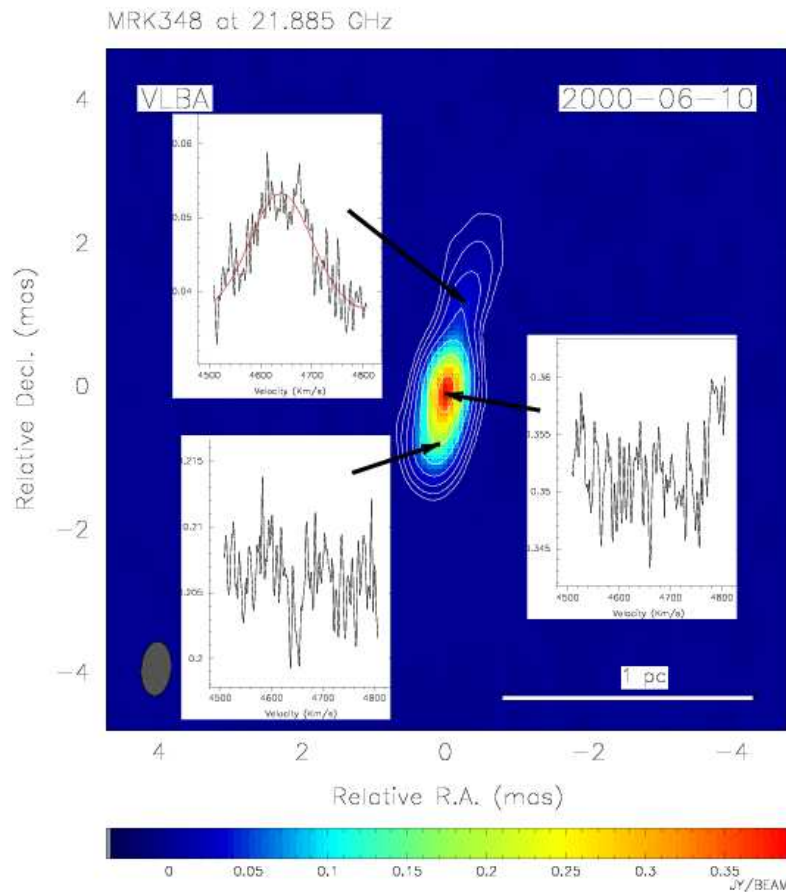


**Figure 3:** Results from VLBA observations of the  $\text{H}_2\text{O}$  maser emission in Mrk 348. The emission is concentrated toward the northern jet [50].

#### 4. Summary and future prospects

VLBI observations have been crucial for improving our understanding of megamasers. Both OH and H<sub>2</sub>O megamasers display very compact structures, and therefore they require VLBI resolution in order to be resolved. VLBI mapping has clearly shown that OH megamasers are associated with the nuclear regions of ULIRGs, and the emission is distributed in circumnuclear structures of scales of about 100 pc. Ongoing theoretical and observational efforts are investigating why some OH emission is found on very small scales with very large line widths. Answers to unsolved questions like why we do not see OH megamasers in every ULIRG may be important for the proposed possibility of using the OH megamasers as a tracer of the merger rate as a function of cosmic time.

H<sub>2</sub>O megamasers are found on much smaller scales, most often in sub-pc accretion disks. VLBI mapping and monitoring of such disks might allow using the H<sub>2</sub>O megamasers for measuring geometric extragalactic distances. However, with the increasing sensitivity of telescopes, other and different types of extragalactic H<sub>2</sub>O masers are being discovered. In particular, a class of weaker extragalactic masers (“kilomasers”), probably associated with star formation, is known to exist [39, 53], although not discussed in this review. Equally exciting is a very recent discovery of a 183-GHz H<sub>2</sub>O megamaser in Arp 220 [12]. These new masers are likely to open up a new field of study of weaker maser emission in extragalactic sources.

#### References

- [1] Araya, E., Baan, W.A., & Hofner, P., 2004, *ApJS*, 154, 541
- [2] Baan, W.A., Guesten, R., & Haschick, A.D., 1986, *ApJ*, 305, 830
- [3] Baan, W.A., Wood, P.A.D., & Haschick, A.D., 1982, *ApJ*, 260, L49
- [4] Baan, W.A., & Klöckner, H.-R., 2006, *A&A*, 449, 559
- [5] Baan, W.A., 1985, *Nature*, 315, 26
- [6] Bialecki, A., Lonsdale, C., Diamond, P., & Thrall, H., 2005, *AAS*, 207, 2110
- [7] Braatz, J.A., Wilson, A.S., & Henkel, C., 1997, *ApJS*, 110, 321
- [8] Braatz, J.A., Wilson, A.S., & Henkel, C., 1996, *ApJS*, 106, 51
- [9] Braatz, J.A., Wilson, A.S., & Henkel, C., 1994, *ApJS*, 437, L99
- [10] Briggs, F.H., 1998, *A&A*, 336, 815
- [11] Burdiuzha, V.V., Vikulov, K.A., 1990, *MNRAS*, 244, 86
- [12] Cernicharo, J., Pardo, J.R., & Weiss, A., 2006, *ApJ*, 646, L49
- [13] Claussen, M.J., Diamond, P.J., Braatz, J.A., Wilson, A.S., Henkel, C., 1998, *ApJ*, 500, L129
- [14] Claussen, M.J., & Lo, K.-Y., 1986, *ApJ*, 308, 592
- [15] Claussen, M.J., Heiligman, G.M., & Lo, K.Y., 1984, *Nature*, 310, 298
- [16] Condon, J.J., Huang, Z.-P., Yin, Q.F., & Thuan, T.X., 1991, *ApJ*, 378, 65
- [17] Darling, J., 2005, *ASPC*, 340, 216
- [18] Darling, J., & Giovanelli, R., 2002, *AJ*, 124, 100

- [19] Darling, J. & Giovanelli, R., 2002, *ApJ*, 569, L87
- [20] Diamond, P.J., Lonsdale, C.J., Lonsdale, C.J., & Smith, H.E., 1999, *ApJ*, 511
- [21] Dos Santos, P.M., & Lepine, J.R.D., 1979, *Nature*, 278, 34
- [22] Freedman, W.L., et al., 2001, *ApJ*, 553, 562
- [23] Gallimore, J.F., Henkel, C., Baum, S.A., Glass, I.S., Claussen, M.J., Prieto, M.A., & Von Kap-herr, A., 2001, *ApJ*, 556, 694
- [24] Gallimore, J.F., Baum, S.A., O’Dea, C.P., Brinks, E., & Pedlar, A., 1996, *ApJ*, 462, 740
- [25] Gardner, F.F., & Whiteoak, J.B., 1982, *MNRAS*, 201, 13
- [26] Greenhill, L.J., 2004, *NewAR*, 48, 1079
- [27] Greenhill, L.J., Booth, R.S., Ellingsen, S.P., Herrnstein, J.R., Jauncey, D.L., McCulloch, P.M., Moran, J.M., Norris, R.P., Reynolds, J.E., & Tzioumis, A.K., 2003, *ApJ*, 590, 162
- [28] Greenhill, L., 2002, *IAUS*, 206, 381
- [29] Greenhill, L.J., & Gwinn, C.R., 1997, *Ap&SS*, 248, 261
- [30] Greenhill, L.J., Moran, J.M., & Herrnstein, J.R., 1997, *ApJ*, 481, L23
- [31] Greenhill, L.J., Henkel, C., Becker, R., Wilson, T.L., & Wouterloot, J.G.A., 1995, *A&A*, 304, 21
- [32] Haschick, A.D., Baan, W.A., & Peng, E.W., 1994, *APJ*, 437, L35
- [33] Haschick, A.D., & Baan, W.A., 1990, *ApJ*, 355, L23
- [34] Haschick, A.D., & Baan, W.A., 1985, *Nature*, 314, 144
- [35] Henkel, C., & Braatz, J.A., 2003, *AcASn*, 44, 55
- [36] Henkel, C., Güsten, R., & Baan, W.A., 1987, *A&A*, 185, 14
- [37] Henkel, C., Güsten, R., Downes, D., Thum, C., Wilson, T.L., & Biermann, P., 1984, *A&A*, 141, L1
- [38] Herrnstein, J.R., Moran, J.M., Greenhill, L.J., Diamond, P.J., Inoue, M., Nakai, N., Miyoshi, M., Henkel, C., & Riess, A., 1999, *Nature*, 400, 539
- [39] Ho, P.T.P., Martin, R.N., Henkel, C., & Turner, J.L., 1987, *ApJ*, 320, 663
- [40] Hu, W., 2005, *Phys. Rev. D* 71, 047301
- [41] Humphreys, E.M.L., Argon, A.L., Greenhill, L.J., Moran, J.M., & Reid, M.J., 2005, *AAS, ASPC*, 340,466
- [42] Klöckner, H.-R., Baan, W.A., & Garrett, M.A., 2003, *Nature*, 421, 821
- [43] Lo, K.Y., 2005, *ARA&A*, 43, 625
- [44] Lonsdale, C.J., Lonsdale, C.J., Diamond, P.J., & Smith, H.E., 1998, *ApJ*, 493, L13
- [45] Miyoshi, M., Moran, J., Herrnstein, J., Greenhill, L., Nakai, N., Diamond, P., & Inoue, M., 1995, *Nature*, 373, 127
- [46] Montgomery, A.S., & Cohen, R.J., 1992, *MNRAS*, 254, 23
- [47] Nakai, N., Inoue, M., & Miyoshi, M., 1993, *Nature*, 361, 45
- [48] Norris, R.P., Baan, W.A., Haschick, A.D., Diamond, P.J., & Booth, R.S., 1985, *MNRAS*, 213, 821



- [49] Parra, R., Conway, J.E., Elitzur, M., & Pihlström, Y.M., 2005, *A&A*, 443, 383
- [50] Peck, A.B., Henkel, C., Ulvestad, J.S., Brunthaler, A., Falcke, H., Elitzur, M., Menten, K.M., & Gallimore, J.F., 2003, *ApJ*, 590, 149
- [51] Polatidis, A.G., & Aalto, S., 2000, in 'Proceedings of the 5th European VLBI Network Symposium', J.E. Conway, A.G. Polatidis, R.S. Booth & Y.M. Pihlström (eds.), published Onsala Space Observatory, p. 129
- [52] Richards, A.M.S., Knapen, J.H., Yates, J.A., Cohen, R.J., Collett, J.L., Wright, M.M., Gray, M.D., & Field, D., 2005, *MNRAS*, 364, 353
- [53] Tarchi, A., Henkel, C., Peck, A.B., & Menten, K.M., 2002, *A&A*, 389, L39
- [54] Vignali, C., Brandt, W.N., Comastri, A., & Darling, J., 2005, *MNRAS*, 364, 99
- [55] Yates, J.A., Richards, A.M.S., Wright, M.M., Collett, J.L., Gray, M.D., Field, D., & Cohen, R.J., 2000, *MNRAS*, 317, 28